The Japan Society of Mechanical Engineers



# Temperatures of Positively and Negatively Stretched Flames*

Kazuhiro YAMAMOTO** and Satoru ISHIZUKA***

Both tubular flame temperature and Bunsen flame temperature have been measured for lean methane, hydrogen and propane/air mixtures. These temperatures have been compared with the adiabatic flame temperature, which is the typical temperature with no stretch. Results show that, the temperature of the tubular flame is almost the same as the adiabatic flame temperature for a lean methane/air mixture, considerably higher for a lean hydrogen/air mixture, and lower for a lean propane/air mixture. For the temperature around the Bunsen flame tip, this response is opposite to that of the tubular flame. To examine radiation effect, numerical simulation has been conducted. It is found that the radiative heat loss only reduces the flame temperature by 30 to 80°C. Thus, the different dependency of flame temperature on the mixtures is explained by stretch effect with the Lewis number considerations, and the response of these flames exhibits opposite behavior.

***Key Words***: Premixed Combustion, Stretch, Swirling Flow, Flame Temperature, Lewis Number, Chemical Equilibrium, Thermal Radiation

## 1. Introduction

Turbulent combustion has been widely used in practical combustion devices including jet engines to industrial power plants. Since it is very complex phenomenon, fundamental studies for modeling of turbulent combustion are useful to design and improve combustion devices. In these studies, we usually focus on vortex flow[1]-[4]. This is because, in turbulent flow, eddies move randomly back-and-forth across the adjacent fluid layers, and the flow no longer remains smooth and orderly. The diffusivity of turbulence causes rapid mixing and increased rates of momentum, heat, and mass transfer, which is important feature of turbulent combustion. Turbulence is swirling, characterized by high levels of fluctuating vorticity. The vortex plays an important role in the turbulent combustion. Thus, the studies on flames in the vortex flow are very important to understand the turbulent combustion phenomena.

We have focused on a tubular flame to investigate the behavior of premixed flames in a vortex flow. Since the tubular flame is formed in a stretched, rotating flow field, the study on this flame yields useful information for turbulent combustion. So far, its extinction limit and flame structure have been examined[5]-[7]. From these studies, it has been found that its characteristics depend on the Lewis number, *Le*, which is defined as the ratio of the thermal diffusivity and the diffusion coefficient of the deficient reactant. For example, the extinction limits depend on Lewis number[5],[6]; for a lean mixture whose Lewis number is less than unity, its flammable range becomes wider, whereas for a mixture whose Lewis number is larger than unity, its flammable range becomes narrower. This is because the stream tube across the flame zone is divergent in a stagnation-point flow, so that a part of the heat generated in the reaction zone and a part of each component of the

* Received 10th May, 2002 (No. 02-4079)

** Department of Mechanical Engineering, Faculty of Engineering Toyohashi University of Technology, 1-1 Hibarigaoka, Tempaku, Toyohashi, Aichi 441-8580, Japan. E-mail: yamamoto@mech.tut.ac.jp

*** Department of Mechanical Engineering, Faculty of Engineering, Hiroshima University, 1-4-1 Kagamiyama, Higashi-hiroshima, Hiroshima 739-0046, Japan.



NII-Electronic Library Service

The Japan Society of Mechanical Engineers



mixture pass through the boundary of the stream tube by conduction and diffusion, respectively. Thus, when the flame is formed in a stretched flow, the stretch effect should be taken into account.

Recently, it has been found that radiation effect is also important for flame stability[8],[9]. The heat loss caused by the radiation reduces the flame temperature. Since the flame temperature is largely related with the flame stability, it is necessary to investigate the stretch effect and radiation effect on flames in different mixtures, for discussion on the stability of stretched flames with Lewis number. However, the tubular flame temperature has not yet been measured except for a methane/air mixture[7].

In this study, from the measurement of tubular flame temperatures with various Lewis numbers, we systematically discuss the stretch effect on flame temperature. Lean hydrogen, methane, and propane/air mixtures are used. To examine the radiation effect, we simulate tubular flames with a Planck mean absorption coefficient model[8]. We also measure the temperatures of Bunsen flames. These temperatures are compared with an adiabatic flame temperature by a chemical-equilibrium calculation program developed by the NASA Lewis Center[10]. Since the adiabatic flame temperature is considered to be the typical temperature with no stretch, it is possible to clarify the stretch effect based of the Lewis number consideration.

## 2. Experimental

Figure 1 shows swirl-type burners used in this study, which are called type A and type B burners. Type A in Fig. 1(a) is the so-called swirl-type burner used in previous studies[5]-[7]. Combustible mixtures are introduced tangentially from the center slit of 3 mm width into a glass tube of 19 mm inner diameter, and the burned gas exits from both ends of the burner; a rotating, stretched flow field is obtained inside the burner tube. The glass tube is 120 mm long, and the center slit is 80 mm long. Nitrogen is introduced from the right and left slits of 20 mm long each in order to prevent a diffusion flame of rich mixtures from damaging the burner. Although only lean mixtures are used in this experiment, nitrogen is also introduced at the same mean tangential ejection velocity of combustible mixtures, $V_t$, to obtain a uniform flow field. In most measurements, only type A is used, unless stated otherwise. Type B is the axisymmetric swirl-type burner (Fig. 1(b)), which has been developed in Ref.(11) to examine the flame characteristics in symmetric flow, compared with those by type A. The center slits for premixed mixtures are 1 mm width and 30 mm length. Mixtures

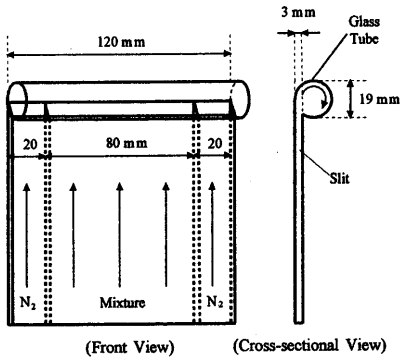


(a) Swirl-type burner (Type A)

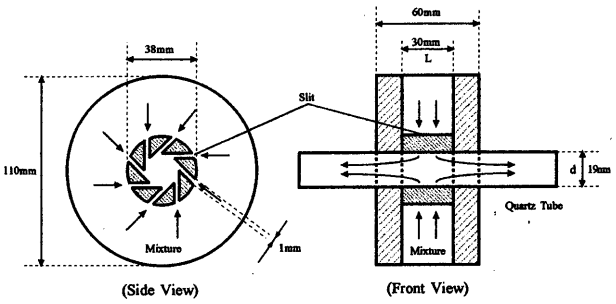


(b) Axisymmetric swirl-type burner (Type B)

Fig. 1 Swirl-type burners used in this study

are introduced through 8 slits to form the axisymmetric flow. Nitrogen is introduced from the right and left slits of 15 mm length. The diameter of the tube is 19 mm, which is the same as that of type A.

For comparison, a Bunsen-type burner is used. This burner has a nozzle giving a uniform velocity distribution at the exit, whose diameter is the same as those of swirl-type burners. A pilot flame is used to stabilize the flame, which is formed on a circular nozzle around the burner exit.

Temperature is measured with a silica coated Pt/Pt-13%Rh thermocouple (wire diameter; 50 μm and 100 μm), which is inserted along the flame front to obtain the flame temperature correctly. In this experiment, since the flame is stable with small turbulence, the temperature fluctuation is very small, except for a polyhedral flame of a lean hydrogen/air mixture. A correction is made for radiative heat loss. The temperature reduction, $\Delta T$, due to the radiation is estimated by considering heat transfer around the bead of the thermocouple by the following equation;

$$\Delta T=\frac{\varepsilon\sigma T^4 D}{\lambda}\frac{1}{Nu}, \qquad (1)$$

where $\varepsilon$ is the emissivity, $\sigma$ is the Stefan-Boltzmann constant, $T$ is the measured temperature, $D$ is the bead diameter, $\lambda$ is the thermal conductivity, and $Nu$ is the Nusselt number. If we put $Nu=0.8\times(Re)^{0.25}$, we obtain the Kaskan's relation[12],



NII-Electronic Library Service

The Japan Society of Mechanical Engineers



$$\Delta T=\frac{1.25\varepsilon\sigma T^4 D^{0.75}}{\lambda}\left(\frac{\eta}{\rho U}\right)^{0.25}, \qquad (2)$$

where $Re$ is the Reynolds number, given by $\rho UD/\eta$, $\eta$ is the viscosity, $\rho$ is the density, and $U$ is the velocity around the bead of thermocouple. If we take $T=927$°C, $D=0.10\times10^{-3}$ m, $U=2.2$ m/s, and $\rho=0.239$ kg/m$^3$ for lean methane/air mixture, and further $\varepsilon=0.23$, $\sigma=5.670\times10^{-8}$ W/m-K$^4$, $\lambda=8.85\times10^{-2}$ W/m-K, and $\eta=4.73\times10^{-5}$ kg/m-s, and put them into Eq.(2), then yielding $\Delta T=37$°C, Since the Reynolds number is very small ($Re=1.11$ in the present case), we assume $Nu=2.0$ (sphere) in Eq.(1), then yielding $\Delta T=33.2$°C. The difference between two values is small, and hence, the correlation is made using Kaskan's relation. Only corrected temperatures are shown in the results, unless stated otherwise.

## 3. Numerical Simulation

In this study, the tubular flame is numerically simulated to examine the radiation effect. Only a methane/air mixture is considered. This effect always exists due to the thermal radiation in combustion, which is different from the radiation loss needed in the temperature measurement by thermocouples. Figure 2 shows the schematic of a tubular flame, with cylindrical coordinates; $z$ and $r$ represent, respectively, longitudinal and radial distance from the center, $\theta$ represents azimuthal angle; $v_r$, $v_\theta$, and $v_z$ represent, respectively, $r$, $\theta$, and $z$ components of the velocity vector $\boldsymbol{v}$. For simplicity of boundary conditions, the wall is rotating to give axially symmetric flow in an infinitely long tube of radius $R$. Then, a similarity solution for the compressible flow can be adopted[13),14]. A combustible mixture is injected through the rotating porous wall, resulting in a uniform velocity vector $\boldsymbol{v}_0(-v_{r,0}, v_{\theta,0}, 0)$ at $r=R$. The component of mixture and the flow velocity at the wall are set to be the experimental values.

Detailed transport coefficients and thermodynamic properties for each species are taken into account. As reaction scheme for a methane/air mixture, we use skeletal mechanism[15]. It consists of 35 elementary reactions and 15 reactive species, $CH_4$, $O_2$, $CO_2$, $H_2O$, CO, $H_2$, H, OH, O, $HO_2$, $CH_3$, CHO, $CH_2O$, $CH_3O$, $H_2O_2$, which are shown in Table 1. Nitrogen is taken as inert. The assumptions and equations in this calculation are identical with those of previous studies[13),14], except that we consider the radiative heat loss by an optically thin radiation model for $CH_4$, $CO_2$, $H_2O$, CO[8]. The tube radius, $R$, is 9.5 mm, which corresponds to burner radius in the experiment. The number of mesh points is 201, and the mesh size is about 0.05 mm, so as to represent the flame structure accurately.

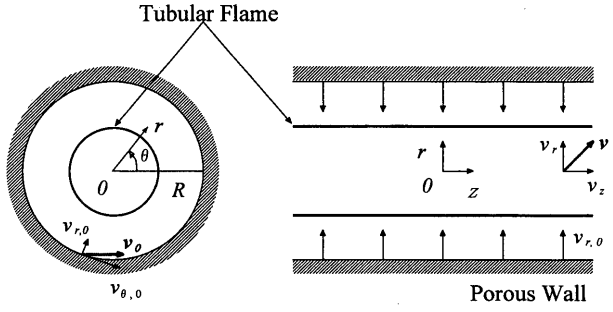


Fig. 2 Axially symmetric flow field in an infinitely long rotating porous tube with uniform injection

## 4. Results

### 4.1 Tubular flame temperature

In our previous study[7], there is a maximum

Table 1 Specific reaction-rate constants for the reaction scheme

| No | Reaction | A | α | E |
|---|---|---|---|---|
| 01 | $H+O_2\rightarrow OH+O$ | 2.00E14 | 0.00 | 70.30 |
| 02 | $OH+O\rightarrow H+O_2$ | 1.57E13 | 0.00 | 2.89 |
| 03 | $H_2+O\rightarrow OH+H$ | 1.80E10 | 1.00 | 36.93 |
| 04 | $OH+H\rightarrow H_2+O$ | 8.00E09 | 1.00 | 28.29 |
| 05 | $H_2+OH\rightarrow H_2O+H$ | 1.17E09 | 1.30 | 15.17 |
| 06 | $H_2O+H\rightarrow H_2+OH$ | 5.09E09 | 1.30 | 77.78 |
| 07 | $OH+OH\rightarrow H_2O+O$ | 6.00E08 | 1.30 | 0.00 |
| 08 | $H_2O+O\rightarrow OH+OH$ | 5.90E09 | 1.30 | 71.26 |
| 09 | $H+O_2+M\rightarrow HO_2+M$ | 2.30E18 | -0.80 | 0.00 |
| 10 | $H+HO_2\rightarrow OH+OH$ | 1.50E14 | 0.00 | 4.20 |
| 11 | $H+HO_2\rightarrow H_2+O_2$ | 2.50E13 | 0.00 | 2.93 |
| 12 | $OH+HO_2\rightarrow H_2O+O_2$ | 2.00E13 | 0.00 | 4.18 |
| 13 | $CO+OH\rightarrow CO_2+H$ | 1.51E07 | 1.30 | -3.17 |
| 14 | $CO_2+H\rightarrow CO+OH$ | 1.57E09 | 1.30 | 93.74 |
| 15 | $CH_4+M\rightarrow CH_3+H+M$ | 6.30E14 | 0.00 | 435.19 |
| 16 | $CH_3+H+M\rightarrow CH_4+M$ | 5.20E12 | 0.00 | -5.48 |
| 17 | $CH_4+H\rightarrow CH_3+H_2$ | 2.20E04 | 3.00 | 36.61 |
| 18 | $CH_3+H_2\rightarrow CH_4+H$ | 9.57E02 | 3.00 | 36.61 |
| 19 | $CH_4+OH\rightarrow CH_3+H_2O$ | 1.60E06 | 2.10 | 10.29 |
| 20 | $CH_3+H_2O\rightarrow CH_4+OH$ | 3.02E05 | 2.10 | 72.90 |
| 21 | $CH_3+O\rightarrow CH_2O+H$ | 6.80E13 | 0.00 | 0.00 |
| 22 | $CH_2O+H\rightarrow CHO+H_2$ | 2.50E13 | 0.00 | 16.70 |
| 23 | $CH_2O+OH\rightarrow CHO+H_2O$ | 3.00E13 | 0.00 | 5.00 |
| 24 | $CHO+H\rightarrow CO+H_2$ | 4.00E13 | 0.00 | 0.00 |
| 25 | $CHO+M\rightarrow CO+H+M$ | 1.60E14 | 0.00 | 61.51 |
| 26 | $CH_3+O_2\rightarrow CH_3O+O$ | 7.00E12 | 0.00 | 107.34 |
| 27 | $CH_3O+H\rightarrow CH_2O+H_2$ | 2.00E13 | 0.00 | 0.00 |
| 28 | $CH_3O+M\rightarrow CH_2O+H+M$ | 2.40E13 | 0.00 | 120.56 |
| 29 | $HO_2+HO_2\rightarrow H_2O_2+O_2$ | 2.00E12 | 0.00 | 0.00 |
| 30 | $H_2O_2+M\rightarrow OH+OH+M$ | 1.30E17 | 0.00 | 190.39 |
| 31 | $OH+OH+M\rightarrow H_2O_2+M$ | 9.86E14 | 0.00 | -21.22 |
| 32 | $H_2O_2+OH\rightarrow H_2O+HO_2$ | 1.00E13 | 0.00 | 7.53 |
| 33 | $H_2O+HO_2\rightarrow H_2O_2+OH$ | 2.86E13 | 0.00 | 137.21 |
| 34 | $H+OH+M\rightarrow H_2O+M$ | 2.20E22 | -2.0 | 0.00 |
| 35 | $H+H+M\rightarrow H_2+M$ | 1.80E18 | -1.0 | 0.00 |

The reaction constants are written as $k=AT^\alpha \exp(-E/R_uT)$, with the individual quantities expressed in cm, mol, s, kJ and K units.
The third-body efficiencies are 0.40 for $O_2$, 6.50 for $H_2O$, 0.40 for $N_2$ and 1.00 for all other species.



NII-Electronic Library Service

The Japan Society of Mechanical Engineers



temperature around the luminous flame region in the radial temperature distribution. This maximum temperature has been defined as the flame temperature. Figure 3 shows the tubular flame temperature for a methane/air mixture using type A, as functions of fuel concentration, $\Omega$ (% volume). For comparison, the flame temperature using type B is shown, which has been already measured[11]. For both cases, the mean tangential ejection velocity, $V_t$, is 3.8 m/s. The temperatures before correlation by Eq.(2) are also shown.

As seen in this figure, the flame temperature monotonically decreases with a decrease of the fuel concentration. The flame extinction occurs when the fuel concentration is 4.84% for type A, and 4.80% for type B. It is interesting to note that both temperatures are almost the same, although type A has only one slit for mixture ejection. Hence, the symmetric assumption adopted in the simulation is valid to discuss the flame characteristics based on numerical results.

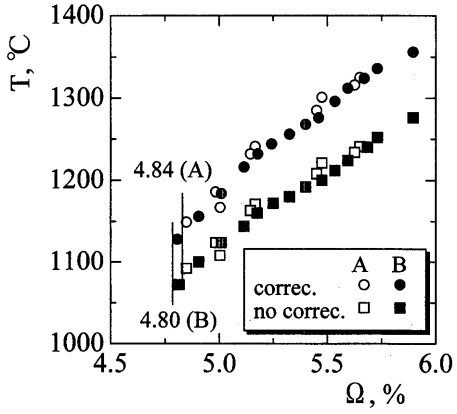


Fig. 3 Variations of flame temperature with fuel concentration, $V_t$=3.8 m/s

Figure 4 shows the variations of the tubular flame temperature with the fuel concentration for hydrogen, methane, and propane/air mixtures. The adiabatic flame temperature, $T_{ad}$, is also shown using the solid line. Although the flame temperature monotonically decreases with a decrease of fuel concentration for all cases, the different response to the adiabatic flame temperature is observed. That is, for a methane/air mixture, the measured flame temperature is almost the same as $T_{ad}$. However, for a hydrogen/air mixture, the flame temperatures are much higher than $T_{ad}$. This temperature difference is about 400°C, which is unexpectedly large. On the contrary, for a propane/air mixture, the flame temperatures are lower than $T_{ad}$ by 50 - 100°C.

### 4.2 Bunsen flame temperature

For comparison, a Bunsen flame is also examined for each mixture. The temperature measurement is conducted about 5 mm downstream from the flame

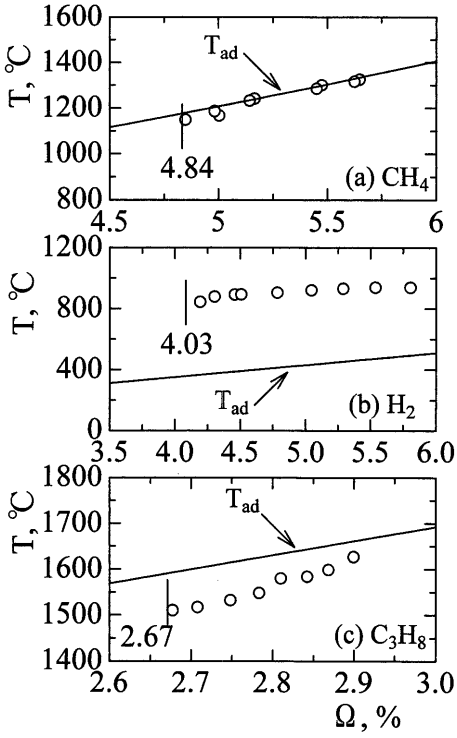


Fig. 4 Comparison between tubular flame temperature and adiabatic flame temperature for (a) methane/air mixtures, (b) hydrogen/air mixtures, (c) propane/air mixtures

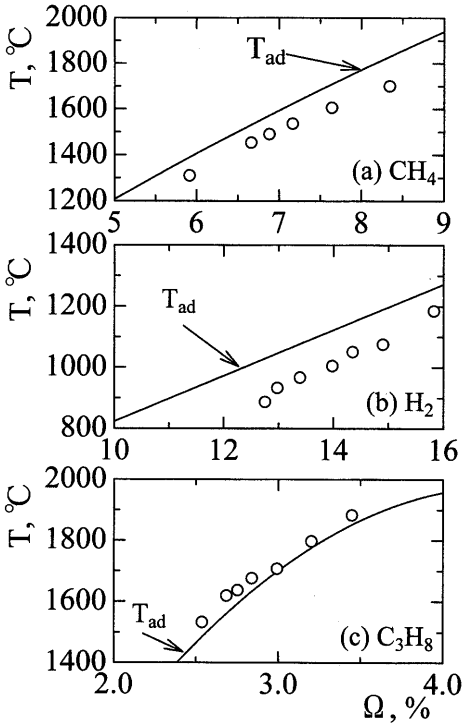


Fig. 5 Comparison between temperature around Bunsen flame tip and adiabatic flame temperature for (a) methane/air mixtures, (b) hydrogen/air mixtures, (c) propane/air mixtures



NII-Electronic Library Service

The Japan Society of Mechanical Engineers



tip. Figure 5 shows the Bunsen flame temperature when the mean exit velocity is set to be 2.2 m/s. The adiabatic flame temperature is also shown. Results show that, for a methane/air mixture, the flame temperature is slightly lower than $T_{ad}$. For a hydrogen/air mixture, as is different from the behavior of the tubular flame, the flame temperature is lower than $T_{ad}$ by 100°C. For a propane/air mixture, the flame temperature is slightly higher than $T_{ad}$. These results are in accordance with the previous experiments[16),(17)]. Therefore, it is found that the Bunsen flame shows different behavior from that of the tubular flame.

For a hydrogen/air mixture, the flame is wrinkling to form a polyhedral flame especially for $\Omega=10.6-17.5\%$, which has been reported in Ref.(18). Here, both luminous and dark regions are observed along the cellular flame front. Then, we traverse the thermocouple at half height of the flame, and measure the temperatures in these regions. Results are shown in Fig. 6. For comparison, the temperature at the flame tip is also obtained, together with adiabatic flame temperature. As seen in this figure, it is found that the temperature in the luminous region is higher than that at the flame tip, while the temperature in the dark region is lower. It is interesting to note that the temperature in the luminous region slightly exceeds the adiabatic flame temperature, which is the same tendency of tubular flames in Fig. 4(b).

## 5. Discussion

Using two swirl-type burners of type A and B, the temperature of the tubular flame in a stretched, rotating flow has been measured for lean methane, hydrogen and propane/air mixtures. The flame temperature on the Bunsen burner has been also measured. These temperatures have been compared with the adiabatic flame temperature.

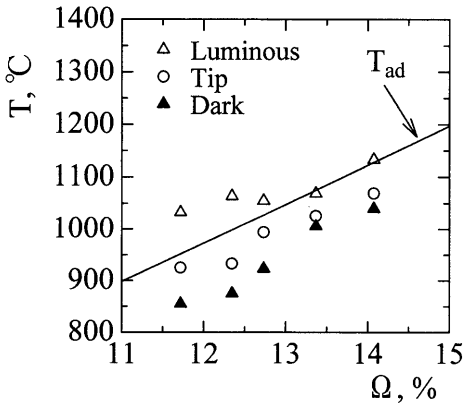


Fig. 6 Comparison between temperature of polyhedral burner flame (luminous, dark and tip regions) and adiabatic flame temperature for hydrogen/air mixtures

From these results, it is found that the tubular flame temperature is almost the same as the adiabatic flame temperature for a lean methane/air mixture, considerably higher for a lean hydrogen/air mixture, and lower for a lean propane/air mixture. It is also found that this response is different from that of the Bunsen flame; the temperature around the flame tip becomes lower than the adiabatic flame temperature by 50°C for a lean methane/air mixture, lower by 100°C for a lean hydrogen/air mixture, and slightly higher for a lean propane/air mixture.

Before discussing these results, we focus on two effects, radiation effect and stretch effect. The radiation effect is discussed first, followed by the stretch effect.

### 5.1 Radiation effect

To estimate the radiation effect quantitatively, we simulate the tubular flame with and without radiation term in the conservation equation of energy. Figure 7 shows the radial distribution of temperature for a methane/air mixture. The fuel concentration is 5.2% and the mean tangential velocity is 3.8 m/s, which corresponds to the experimental condition. The rotating porous wall is located at $r=9.5$ mm. When radiative heat loss is not considered, shown by solid line, the temperature starts to increase at $r=5$ mm, and steeply increases in the reaction zone, which is located at $r=2-4$ mm. The temperature takes its maximum at $r=0$ mm. With radiative heat loss, the temperature profile is similar, but the maximum temperature is lower by 60°C. The maximum temperature is located around the reaction region, which corresponds to the experiments[7].

Then, we compare the calculated temperature with temperatures obtained by type A and B burners. Figure 8 shows the variations of flame temperature with fuel concentration. As seen in this figure, it is

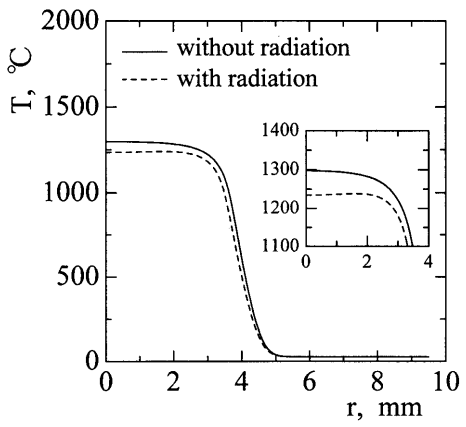


Fig. 7 Temperature distribution for methane/air mixtures obtained by numerical simulation, $\Omega=5.2\%$, $V_t=3.8$ m/s



NII-Electronic Library Service

The Japan Society of Mechanical Engineers



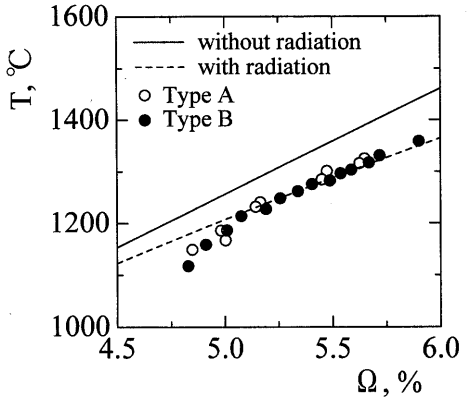


Fig. 8 Comparison between tubular flame temperature and calculated flame temperature with and without radiative heat loss for methane/air mixtures

found that the flame temperature with radiation loss is always lower than that without radiation by 30 - 80°C. The temperature difference is smaller as the fuel concentration is decreased. This is explained by the fact that the radiative heat loss is proportional to the fourth power of the temperature. As the fuel concentration is smaller, the radiation effect is reduced with the lower flame temperature. It is also due to the fact that the mole fraction of radiating species such as $CO_2$ and $H_2O$ is smaller with an decrease of the fuel concentration.

It should be noted that the calculated flame temperature with radiation loss is almost the same as the experimentally obtained flame temperature. Then, radiation loss must be included to predict the flame temperature accurately. However, in Fig. 4, even if the radiation loss is taken into account, the tubular flame temperature is much higher than $T_{ad}$ for a hydrogen/air mixture, whereas the tubular flame temperature is lower than $T_{ad}$ for a propane/air mixture.

Since the tubular flame is formed in stretched flow, the flame characteristics including the flame temperature could be explained with Lewis number considerations, focusing on the mass and heat transfer through flow-divergence. The typical Lewis numbers are 0.31 for 5% hydrogen, 1.7 for 2.8% propane, and 0.95 for 5% methane. Comparing with the Bunsen flame, the dependence of the flame temperature on the Lewis number is clearly observed in Table 2, taking the radiation loss into account. It should be noted that the tubular flame exhibits qualitatively opposite behavior to that of Bunsen flame. Therefore, we estimate the stretch rate of these flames for further discussion.

### 5.2 Stretch effect

In general, the stretch rate, $\kappa$, is given by the following equation[19),(20)].

Table 2 Flame temperature, $T_f$, and adiabatic temperature, $T_{ad}$

| Mixture | Tubular Flame | Bunsen Flame |
|---|---|---|
| $H_2$/Air (Le<1) | $T_f \gg T_{ad}$ | $T_f < T_{ad}$ |
| $CH_4$/Air (Le≈1) | $T_f \approx T_{ad}$ | $T_f \approx T_{ad}$ |
| $C_3H_8$/Air (Le>1) | $T_f \ll T_{ad}$ | $T_f > T_{ad}$ |

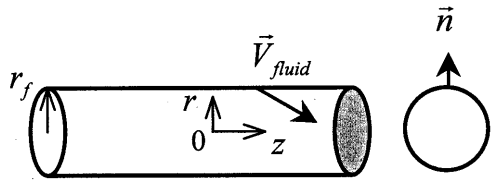


(a) Tubular flame

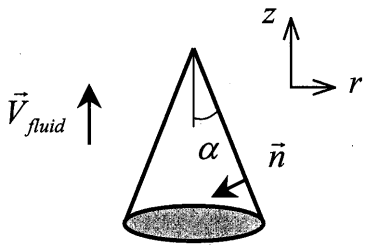


(b) Bunsen flame

Fig. 9 Flame and flow configuration

$$\kappa=\frac{1}{\delta A}\frac{d(\delta A)}{d\tau}$$
$$=-\{\nabla\times(\vec{V}_{\text{fluid}}\times\vec{n})\}\cdot\vec{n}+(\vec{v}\cdot\vec{n})(\nabla\cdot\vec{n})$$
$$=-\{\nabla\times(\vec{V}_{\text{fluid}}\times\vec{n})\}\cdot\vec{n}+(S_L+\vec{V}_{\text{fluid}}\vec{n})(\nabla\cdot\vec{n}) \quad (3)$$

Then, the stretch rate is described by two terms. In Eq.(3), the first is the strain term, and the second is the curvature term. For the tubular flame in Fig. 9 (a), by assuming that the flame is rigorously cylindrical[21], the velocity vector of the flow and the normal vector of the flame front are roughly expressed as:

$$\vec{V}_{\text{fluid}}=(v_r, v_\theta, v_z)=\left(-\frac{1}{2}a\cdot r, 0, a\cdot z\right)$$
$$\vec{n}=(1, 0, 0)$$

Here, $a$ is the axial velocity gradient. If the flame is located at $r=r_f$, the burning velocity becomes $(a/2)\cdot r_f$. With these values,

$$(\kappa)_{\text{Tubular}}=-\vec{n}\vec{n}:\nabla\vec{V}_{\text{fluid}}+\nabla\cdot\vec{V}_{\text{fluid}}+S_L\nabla\cdot\vec{n}$$
$$=\frac{a}{2}+0+S_L\frac{1}{r_f}$$
$$=\frac{a}{2}+\frac{a}{2}=a \quad (4)$$

Resultantly, the stretch rate is $a$, and the flame is formed in positively stretched flow. The estimated value of $a$ in this experiment is about 40 1/s.



NII-Electronic Library Service

The Japan Society of Mechanical Engineers



In case of the Bunsen flame, for simplicity, it is assumed that the flame is formed in uniform flow (Fig. 9(b)). When the flow velocity is $U$ and the crossing angle between flame and flow is $\alpha$, the velocity vector of the flow and the normal vector of the flame front are:

$$\vec{V}_{\text{fluid}}=(v_r, v_\theta, v_z)=(0, 0, U)$$
$$\vec{n}=(-\cos\alpha, 0, -\sin\alpha)$$

Then, the burning velocity is considered to be $U\cdot\sin\alpha$. With these values, the stretch rate for the Bunsen flame is:

$$(\kappa)_{\text{Bunsen}}=0+0+S_L\nabla\cdot\vec{n}$$
$$=U\sin\alpha\frac{1}{r}\frac{\partial}{\partial r}\{r(-\cos\alpha)\}$$
$$=-\frac{U\sin\alpha\cos\alpha}{r} \quad (5)$$

Hence, the Bunsen flame receives negative stretch. For typical case, the estimated stretch rate is about $-20$ 1/s. Therefore, the different characteristics of temperatures between the tubular flame and the Bunsen flame are attributed to the stretch effect.

In Fig. 10, we show the flame and flow configurations to explain the transport of mass and heat. As seen in Fig. 10(a), the flow in the Bunsen flame is uniform while its flame front is curved. Then, there is transport of mass and heat across the flame zone. Since it is a fuel lean mixture, around the flame tip, the mass transport by diffusion increase the concentration of the fuel, the deficient reactant, to intensify the combustion reaction. While, the heat transport by conduction reduces the combustion reaction. In Fig. 10(b), the flow in the tubular flame is divergent while its flame front is flat. Then, the stream tube across the flame zone is divergent, so that a part of the heat generated in the reaction zone and a part of each component of the mixture pass through the boundary of the stream tube by conduction and diffusion, respectively. In both cases, the flame characteristics depend on the Lewis number. From the simple estimation, the Bunsen flame receives negative stretch, and the tubular flame receives positive stretch. Therefore, the different dependency of flame temperature on the mixtures is explained with the Lewis number considerations. Since the stretch rate for these flames is opposite, the tubular flame and the Bunsen exhibit qualitatively opposite behavior.

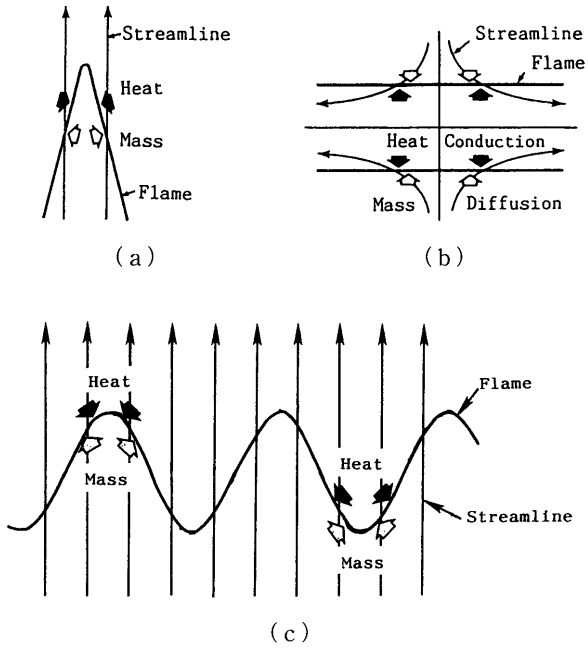


Fig. 10 Schematics illustrating the directions of heat conduction and mass diffusion of limiting reactant in various flames: (a) Bunsen flame, (b) tubular flame, and (c) cellular flame

In the polyhedral flame on the Bunsen burner for a lean hydrogen/air mixture, the temperature in the luminous region is higher than adiabatic flame temperature. This result is also explained with the stretch effect, because the cellular flame has a curved flame front. Hydrogen, a deficient species for lean mixture, diffuses preferentially into the luminous region and the temperature increases, which is shown in Fig. 10 (c). Note that the luminous region is convex towards the unburned mixture stream and hence stretch is positive as in the tubular flame, while the dark region is concave towards the unburned mixture stream, resulting in negative stretched flame. Hence, the temperature of the polyhedral flame in Fig. 6 is also explained with the stretch effect.

In Fig. 11, the Bunsen flame temperatures for luminous and dark regions are compared with that of the tubular flame for a hydrogen/air mixture. As shown by dashed line, the tubular flame temperature and the Bunsen flame temperature in the luminous region show the same linear dependence on the fuel

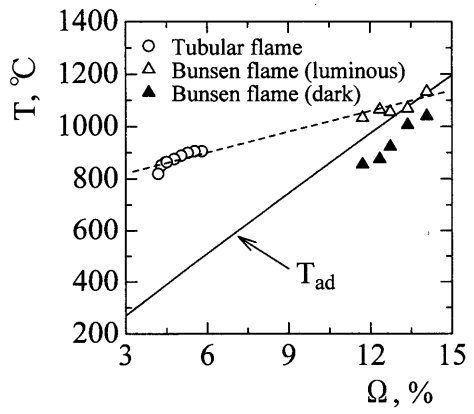


Fig. 11 Comparison between tubular flame temperature, temperature of polyhedral burner flame (luminous, dark regions), and adiabatic flame temperature for hydrogen/air mixtures



NII-Electronic Library Service

The Japan Society of Mechanical Engineers



concentration. Thus, it appears that the tubular flame corresponds to this intensified combustion region of the polyhedral flame, and both are higher than the adiabatic flame temperature.

## 6. Conclusions

Both tubular flame temperature and Bunsen flame temperature have been measured for lean methane, hydrogen and propane/air mixtures. These temperatures have been compared with the adiabatic flame temperature, which is the typical temperature with no stretch. Results show that, the temperature of the tubular flame is almost the same as the adiabatic flame temperature for a lean methane/air mixture, considerably higher for a lean hydrogen/air mixture, and lower for a lean propane/air mixture. For the temperature around the Bunsen flame tip, this response is opposite to that of the tubular flame. Numerical simulation has been conducted to examine the radiation effect, and the flame temperature is well predicted if the radiation loss is taken into account. It is found that the radiative heat loss only reduces the flame temperature by 30 to 80°C. From the simple consideration of the flame and flow configurations, the tubular flame receives a positive stretch, while the Bunsen flame receives a negative stretch. Therefore, the different dependency of flame temperature on the mixtures is explained by the stretch effect with the Lewis number considerations, and the response of these flames exhibits qualitatively opposite behavior.

## References


(1) Robert, W.L. and Driscoll, J.F., Combust. Flame, Vol. 87 (1991), pp. 245-256.

(2) Poinsot, T., Veynante, D. and Candel, S., Proc. Comb. Inst., Vol. 23 (1990), pp. 613-619.

(3) Ashurst, W.T. and McMurtry, P.A., Comb. Science and Technology, Vol. 66 (1989), pp. 17-37.

(4) Peters, N. and Williams, F.A., Proc. Comb. Inst., Vol. 22 (1988), pp. 495-503.

(5) Ishizuka, S., Proc. Comb. Inst., Vol. 20 (1984), pp. 287-294.

(6) Ishizuka, S., Combustion and Flame, Vol. 75, No. 367 (1989).

(7) Yamamoto, K., Ishizuka, S. and Hirano, T., Proc. Comb. Inst., Vol. 25 (1994), pp. 1399-1406.

(8) Ju. Y., Guo, H., Maruta, K. and Liu, F., J. Fluid Mech., Vol. 342 (1997), pp. 315-334.

(9) Ju, Y., Masuya, G., Liu, F., Guo, H., Maruta, K. and Niioka, T., Proc. Comb. Inst., Vol. 27 (1998), pp. 2551-2557.

(10) Gordon, S. and McBride, B.J., NASA SP-273 Interim Revision N78-17724, (1976).

(11) Yamamoto, K. and Ishizuka, S., Trans. Jpn. Soc. Mech. Eng., (in Japanese), Vol. 62, No. 600, B (1996), pp. 3185-3190.

(12) Kaskan, W.E., Proc. Comb. Inst., Vol. 6 (1957), pp. 134-143.

(13) Yamamoto, K., Ishizuka, S. and Hirano, T., Proc. Comb. Inst., Vol. 26 (1996), pp. 1129-1135.

(14) Yamamoto, K., Combust. Flame, Vol. 118 (1999), pp. 431-444.

(15) Rogg, B., Lecture Notes in Physics, Vol. 384 (1991), pp. 159-192, Springer-Verlag.

(16) Mizomoto, M., Asaka, Y., Ikai, S. and Law, C.K., Proc. Comb. Inst., Vol. 20 (1984), pp. 1933-1939.

(17) Law, C.K., Cho, P., Mizomoto, M. and Yoshida, H., Proc. Comb. Inst., Vol. 21 (1986), pp. 1803-1809.

(18) Lewis, B. and von Elbe, G., Combustion, Flames and Explosions of Gases, 3rd Edn., (1987), p. 322, Academic Press.

(19) Matalon, M., Combustion Science and Technology, Vol. 31 (1983), pp. 169-181.

(20) Chung, S.H. and Law, C.K., Combust. Flame, Vol. 55 (1984), pp. 123-125.

(21) Ishizuka, S., Prog. Energy Combust. Sci., Vol. 19 (1993), pp. 187-226.




NII-Electronic Library Service